Journal Pre-proofs

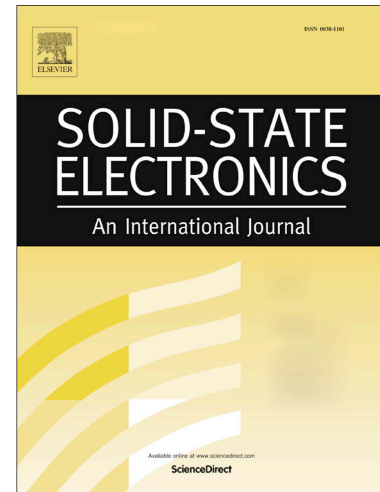

Low-frequency noise in polysilicon Source-Gated Thin-Film transistors

Q. Chen, L.Van Brandt, V. Kilchytska, E. Bestelink, R.A. Sporea, D. Flandre

PII: S0038-1101(25)00044-9
DOI: https://doi.org/10.1016/j.sse.2025.109099
Reference: SSE 109099

To appear in: *Solid-State Electronics*

Please cite this article as: Chen, Q., Brandt, L.Van, Kilchytska, V., Bestelink, E., Sporea, R.A., Flandre, D., Low-frequency noise in polysilicon Source-Gated Thin-Film transistors, *Solid-State Electronics* (2025), doi: https://doi.org/10.1016/j.sse.2025.109099

This is a PDF file of an article that has undergone enhancements after acceptance, such as the addition of a cover page and metadata, and formatting for readability, but it is not yet the definitive version of record. This version will undergo additional copyediting, typesetting and review before it is published in its final form, but we are providing this version to give early visibility of the article. Please note that, during the production process, errors may be discovered which could affect the content, and all legal disclaimers that apply to the journal pertain.

© 2025 Published by Elsevier Ltd.

Journal Pre-proofs

Low-frequency Noise in Polysilicon Source-Gated Thin-Film Transistors

Q. Chen[a,*], L. Van Brandt[a], V. Kilchytska[a], E. Bestelink[b], R. A. Sporea[b], D. Flandre[a]

[a]*Institute of Information and Communication Technologies, Electronics and Applied Mathematics, UCLouvain,*

Louvain-la-Neuve 1348, Belgium

[b]*Advanced Technology Institute, University of Surrey, Guildford, United Kingdom*

[*]*Corresponding author e-mail address: qi.chen@uclouvain.be*

Abstract **The low-frequency noise (LFN) of thin-film polysilicon source-gated transistors (SGTs) is investigated. DC characteristics were firstly measured and typical behaviors of SGT were observed. Then, TCAD simulations were performed with different doping concentrations. Current density distribution shows that the variation of the conduction channel position in the thin film induces a second plateau in the $(g_m/I_D)^2$ curves for bias points in subthreshold region. LFN was measured for both SGTs and thin-film field-effect transistor (TFTs) configurations. 1/*f* noise is confirmed as the main component of LFN in all our measurements. Carrier mobility fluctuation (CMF) is found to dominate the origin of LFN in TFT configuration and the low-current region of SGT. In the high-current region of SGT measurements, 1/*f* noise is mainly attributed to carrier number fluctuation (CNF).**

Key words: low-frequency noise, polysilicon TFT, source-gated transistors, carrier mobility fluctuation, carrier number fluctuation

1. Introduction

In thin-film field-effect transistors (TFTs) intended for high-voltage operation, e.g. for large-area display or analog circuit applications, a new type of device named Source-Gated Transistors (SGTs) [1] provides many advantages, such as reduced short-channel effects, low saturation voltage and high intrinsic gain [2]. By intentionally overlapping the gate with a Schottky, or rectifying, source contact (as well as ensuring the active layer can be fully depleted by the reverse biased barrier during operation), SGTs have been extensively studied with various device architectures [3] and different channel materials including polysilicon [4], organic [5], and metal oxide semiconductors [6]. Among them, low-temperature-processed polysilicon is often favored for its balanced cost and electrical performance suitable for circuit applications such as thin-film large-area displays.

Low-frequency noise (LFN), notably 1/*f* or flicker noise, has always been an important concern for analog circuits that require high precision, stability, or resolution [7]. LFN noise has already been widely studied in many thin-film transistors [8], as well as fully-depleted silicon-on-insulator (FDSOI) transistors [9].

To the best of our knowledge, the noise in SGTs has not been studied yet, but is of interest, given that SGTs are promising components for many analog circuit applications, such as amplifiers [10] or temperature sensors [11]. In this work, the LFN of polysilicon SGTs is investigated. Transfer and output characteristics were measured. TCAD simulations were used to reveal the current transport mechanism of SGTs and explain the second plateau observed in the $(g_m/I_D)^2$ curves. Noise measurements were performed on the same device structure in both TFT and SGT configurations. Two 1/*f* models notably related to carrier mobility fluctuation and carrier number fluctuation are finally used to analyze the experimental noise characteristics.

2. Results and discussion

2.1. DC characteristics of polysilicon SGTs

The schematic cross-section of the device under test is shown in Fig. 1(a) [4]. The device width, channel region length (d) – defined as source-drain distance – and source-gate overlap length (S) are 50, 4 and 4 µm,

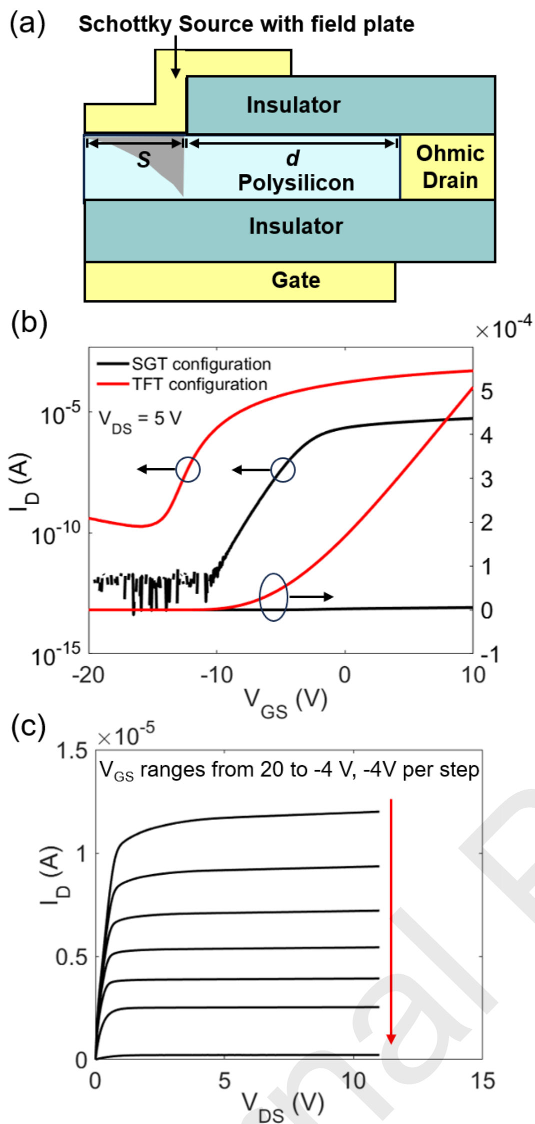

Fig.1. (a) Schematic cross-section of the polysilicon SGT [4]. Depletion region caused by the Schottky barrier is shown as the gray area. (b) Transfer curves for SGT and TFT configurations at V_{DS} = 5 V. (c) Output characteristics under different gate voltages. Here the n-type polysilicon layer doping dose is 0.5×10^{12} cm^{-2}.

Journal Pre-proofs

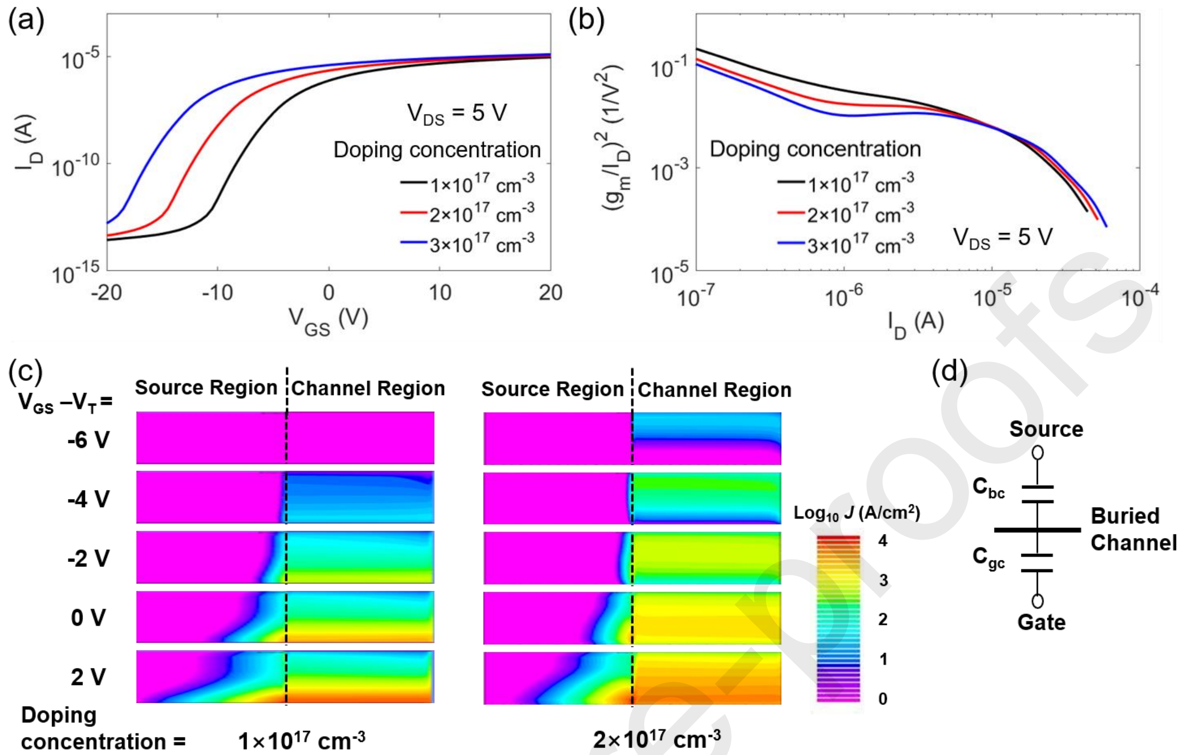

Fig.2. (a) TCAD transfer and (b) $(g_m/I_D)^2$ versus I_D curves of polysilicon SGTs simulated for different doping concentrations. V_{DS} = 5 V. (c) The current densities in the channel and below source region with increased V_{GS}-V_T of 1×10^{17} and 2×10^{17} cm^{-3} doping concentrations, respectively. (d) Simplified capacitance model of the accumulation-mode subthreshold operation.

respectively [4]. The polysilicon layer is deposited at low temperature, 40 nm thick and n-type doped. The bottom gate insulator has an effective oxide thickness of 120 nm. In this study, SGT configuration for device measurements uses chromium to form a Schottky source contact with polysilicon and heavy n-type doping to form an Ohmic drain. TFT configuration was obtained by just swapping the source and drain terminals. The device transfer and output curves are illustrated in Fig. 1(b) and (c) for both SGT and TFT configurations with doping dose = 0.5×10^{12} cm^{-2}. From the I-V characteristics, using the equation presented in [12], the effective Schottky barrier height is estimated to be about 0.325eV at V_{GS} = 0 V. In Fig. 1 (b), the on-current in the TFT configuration increases by two orders of magnitude compared to the SGT configuration. Note that in the TFT configuration, the forward biased Schottky barrier quickly vanishes for a small V_{DS} and has negligible impact on the LFN. In Fig. 1 (c), at high current, the SGT curves clearly saturate at very low drain voltages (below 1 V) and the output impedances are considerably high, thanks to the pinch-off region under source that is induced by the reverse biased Schottky barrier, which fully depletes the polysilicon under the source-edge (the gray region in Fig. 1 (a)).

The LFN in transistors is usually characterized by S_{ID}, its power spectral density (PSD) on the drain current I_D. A normalized figure-of-merit (FOM) S_{ID}/I_D^2, is often introduced with the form

$$\frac{S_{I_D}}{I_D^2} = \left(\frac{g_m}{I_D^2}\right)^2 S_{V_G}, \qquad (1)$$

for comparison of devices as a function of the bias point, where g_m is the transconductance and S_{VG} is the gate-referred voltage noise PSD.

Considering the $(g_m/I_D)^2$ factor in the noise FOM, the device operation was studied with the Silvaco atlas TCAD tool [13]. The simulated transfer curves and extracted $(g_m/I_D)^2$ curves of SGTs at V_{DS} = 5 V with doping concentrations ranging from 1 to 3×10^{17} cm^{-3} are shown in Fig. 2 (a) and (b), respectively. With increased doping concentrations, the transfer curve shifts toward negative threshold values V_T and the $(g_m/I_D)^2$ curve gradually forms a second plateau in subthreshold region. To explain these behaviors and have a better insight on the current transport mechanism of the devices, we analyzed the current densities in the channel and below the source region of

the SGTs at bias points in the subthreshold and near-threshold regimes for 1×10^{17} and 2×10^{17} cm^{-3} doping concentrations, respectively (Fig.2(c)). For high

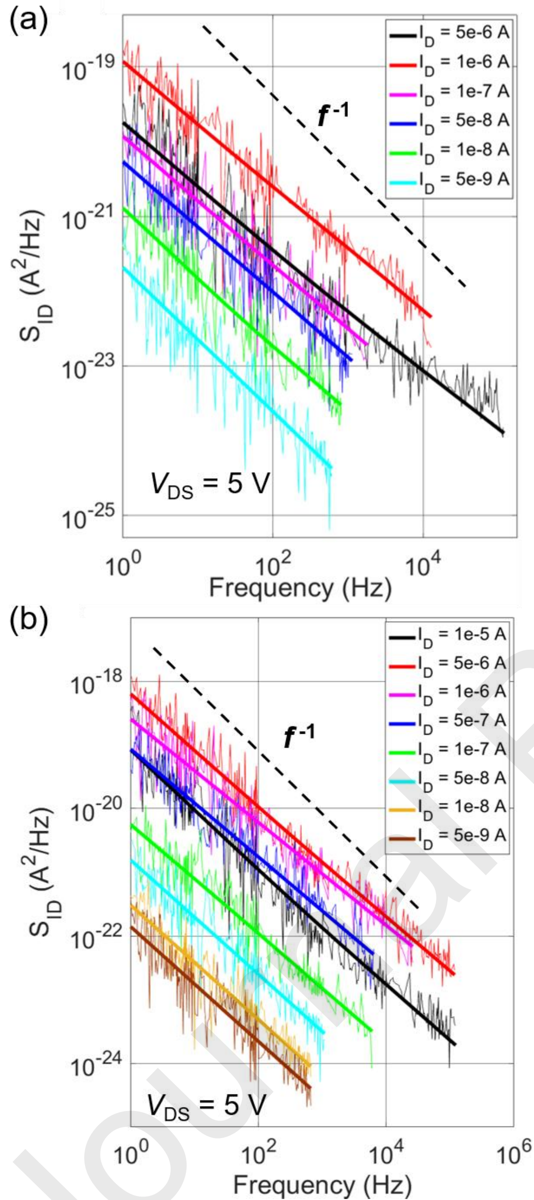

Fig.3 Current noise power spectral densities S_{ID} versus frequency at increased fixed drain current I_D for the SGTs with doping doses = (a) 0.5×10^{12} (b) and 1.5×10^{12} cm^{-2}. V_{DS} = 5 V. Fitted lines of S_{ID} are displayed as well.

doping, the channel firstly forms at the top of the polysilicon layer and slowly moves to the bottom gate with increased V_{GS}-V_T. For low doping, the channel region can be fully depleted for the lower gate bias so that the channel always develops from the bottom gate. The $(g_m/I_D)^2$ can be expressed as a function of the subthreshold slope (SS) :

$$\left(\frac{g_m}{I_D}\right)^2 = \left(\frac{d\ln I_D}{dV_G}\right)^2 = \left(\frac{\ln 10}{SS}\right)^2 \qquad (2)$$

As the subthreshold region of SGT is governed by

the parasitic FET in the channel, SS can be interpreted by a simplified capacitance model of the accumulation-mode transistor (Fig. 2(d)) [14]

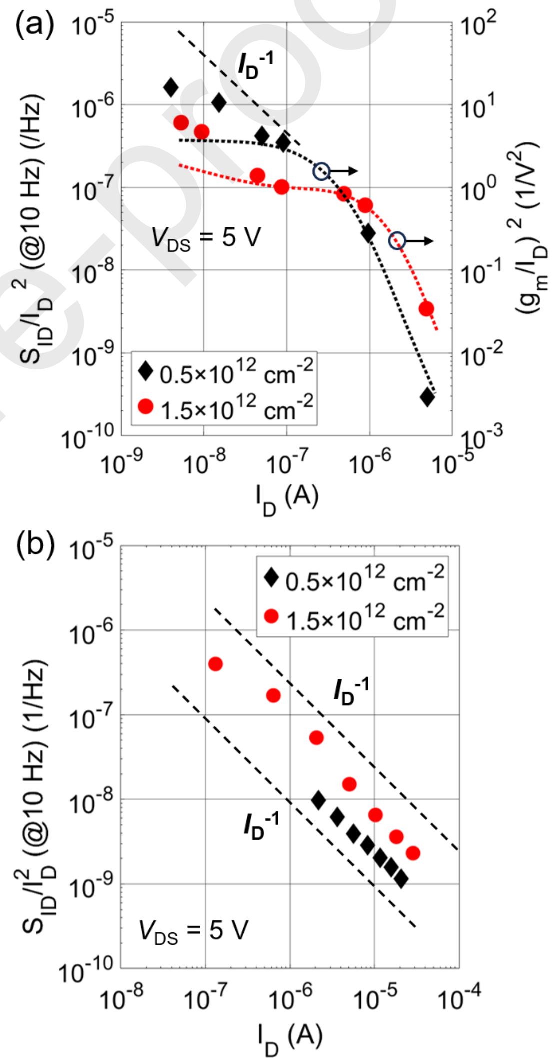

Fig.4 Normalized noise power spectral density S_{ID} / I_D^2 at 10 Hz (dots) as functions of I_D for (a) SGT with Schottky source and (b) counterpart TFT with Ohmic source for 2 different doping doses at V_{DS} = 5 V. The curves of $(g_m/I_D)^2$ and I_D^{-1} (dashed lines) are plotted for comparison.

Journal Pre-proofs

Journal Pre-proofs

$$SS = \ln 10 \frac{kT}{q}\left(1+\frac{C_{\mathrm{bc}}}{C_{\mathrm{gc}}}\right), \qquad (3)$$

where C_{gc} and C_{bc} are the coupling capacitances from gate to channel and channel to source, respectively. For high doping, the intermediate plateau of the SS, and hence g_m/I_D, occurs when the channel is buried in the middle of the thin film. In

comparison, for low doping, g_m/I_D is higher (as C_{gc} is increased and C_{bc} is reduced) and keeps more continuous with bias as is usual.

2.2. LFN characteristics

Fig. 3 (a) and (b) show the S_{ID} of SGTs with increased fixed drain current in subthreshold region for 0.5×10^{12} and 1.5×10^{12} cm^{-2} doping doses, respectively. The curves of S_{ID} as functions of frequency vary approximately proportional to f^{-1}. This confirms that the LFN of the studied SGTs in subthreshold region is mainly contributed by the 1/f noise. The noise contribution of the channel access resistances is assessed to remain negligible since there is no trend of increasing noise in the high I_d region (as shown in Fig. 4)， unliked reported elsewhere [15].

Two models are usually proposed to analyze the LFN noise of transistors. One is the the carrier mobility fluctuation (CMF) model according to which carrier mobility fluctuations are due to phonon scattering effects in the poly-Si channel, given by [16]

$$\frac{S_{\mathrm{I_D}}}{I_{\mathrm{D}}^2} = \frac{q\alpha_{\mathrm{h}}\mu V_{\mathrm{DS}}}{fL^2 I_{\mathrm{D}}}, \qquad (4)$$

where q is the electron charge, μ is mobility, L is the channel length, and α_h is a material dependent parameter, called Hooge parameter. The other is the carrier number fluctuation (CNF) model, which considers the trapping/detrapping of defects at semiconductor/gate oxide interface, given by [16]

$$\frac{S_{\mathrm{I_D}}}{I_{\mathrm{D}}^2} = \left(\frac{g_{\mathrm{m}}}{I_{\mathrm{D}}}\right)^2 \frac{q^2 kT\lambda N_{\mathrm{t}}}{WLC_{\mathrm{OX}}^2 f}, \qquad (5)$$

where k is the Boltzmann constant, T is the temperature, λ is the tunneling attenuation length (≈ 0.1 nm)，N_t is the oxide trap density, W is the device width and C_{OX} is the oxide capacitance per unit area.

Normalized PSD S_{ID}/I_D^2 of SGTs and TFTs as functions of I_D are shown in Fig. 4 (a) and (b), respectively. In Fig. 4(a), the SGT S_{ID}/I_D^2 curves of all doping cases are proportional to the corresponding $(g_m/I_D)^2$ curves in the high-I_D region and to I_D^{-1} in the low-I_D region. According to equations (4) and (5), the LFN of polysilicon SGT originates from the CMF in the low-I_D region and the CNF in the high-I_D region, respectively. In the highly doped device, the $(g_m/I_D)^2$ curve shows an intermediate plateau following the position of buried channel in the film depth as discussed in the TCAD analysis. In Fig. 4(b), the TFT S_{ID}/I_D^2 curves of all doping cases follow the inverse of I_D. This relates the origin of LFN in polysilicon TFTs to CMF, which is consistent with previous studies [17].

3. Conclusion

Our measurements, simulations and analysis, demonstrate that the LFN in polysilicon SGTs and TFTs is dominated by the 1/*f* noise. CMF is found to be the origin of 1/*f* noise in the polysilicon TFTs and in the low-I_D region of polysilicon SGTs, while CNF causes the 1/*f* noise in the high-I_D region of polysilicon SGTs. For the high-doped channel, a second plateau is found in the $(g_m/I_D)^2$ curve in subthreshold region due to the slowly varying position of the buried channel in the very thin polysilicon layer as analyzed by modelling.

The dependence of LFN on some key parameters for polysilicon SGTs, such as source contact length and Schottky barrier height, should be investigated in the future. This study of LFN in SGTs is valuable for analog circuit applications (such as displays and sensors) that requires high resolution, accuracy and stability.

This work was supported by the China Scholarship Council and UCLouvain Co-funding Fellowship (No. CSC202106130093).

References

[1] Shannon JM, Gerstner EG. Source-gated thin-film transistors. IEEE Electron Device Letters 2003;24:405–7. https://doi.org/10.1109/LED.2003.813379.

[2] Wang G, Zhuang X, Huang W, Yu J, Zhang H, Facchetti A, et al. New opportunities for high-performance source-gated transistors using unconventional materials. Advanced Science 2021;8. https://doi.org/10.1002/advs.202101473.

[3] Sporea RA, Jayawardena KDGI, Constantinou M, Ritchie M, Brewin A, Wright W, et al. Heterostructure source-gated transistors: challenges in design and fabrication. ECS Trans 2016;75:61–6. https://doi.org/10.1149/07510.0061ecst.

[4] Sporea RA, Trainor MJ, Young ND, Shannon JM, Silva SRP. Intrinsic gain in self-aligned polysilicon source-gated transistors. IEEE Trans

Electron Devices 2010;57:2434–9. https://doi.org/10.1109/TED.2010.2056151.

[5] Kim Y, Lee EK, Oh JH. Flexible low-power operative organic source-gated transistors. Adv Funct Mater 2019;29. https://doi.org/10.1002/adfm.201900650.

[6] Zhang J, Wilson J, Auton G, Wang Y, Xu M, Xin Q, et al. Extremely high-gain source-gated transistors. Proc Natl Acad Sci U S A 2019;116:4843–8. https://doi.org/10.1073/pnas.1820756116.

[7] Marinov O, Deen MJ, Jiménez-Tejada JA. Low-frequency noise in downscaled silicon transistors: Trends, theory and practice. Phys Rep 2022;990:1–179. https://doi.org/10.1016/j.physrep.2022.06.005.

[8] Yang Y, Zhang M, Lu L, Wong M, Kwok HS. Low-frequency noise in bridged-grain polycrystalline silicon thin-film transistors. IEEE Trans Electron Devices 2022;69:1984–8. https://doi.org/10.1109/TED.2022.3148697.

[9] Van Brandt L, Esfeh BK, Planes N, Kilchytska V, Flandre D. Low-Frequency Noise Transistor Performance for UTBB FDSOI MOSFET-C Filters. 2019 IEEE SOI-3D-Subthreshold Microelectronics Technology Unified Conference, S3S 2019, Institute of Electrical and Electronics Engineers Inc.; 2019. https://doi.org/10.1109/S3S46989.2019.9320711.

[10] Bestelink E, Niang KM, Bairaktaris G, Maiolo L, Maita F, Ali K, et al. Compact source-gated transistor analog circuits for ubiquitous sensors. IEEE Sens J 2020;20:14903–13. https://doi.org/10.1109/JSEN.2020.3012413.

[11] Bestelink E, Teng HJ, Sporea RA. Contact doping as a design strategy for compact TFT-based temperature sensing. IEEE Trans Electron Devices 2021;68:4962–5. https://doi.org/10.1109/TED.2021.3106276.

[12] Shannon JM. Thermionic-field emission through silicon Schottky barriers at room temperature. Solid State Electron 1977;20:869–72. https://doi.org/10.1016/0038-1101(77)90176-9.

[13] Atlas user's manual: device simulation software. Santa Clara, CA,: Silvaco Inc.; 2015.

[14] Rudenko T, Kilchytska V, Colinge J-P, Dessard V, Flandre D. On the high-temperature subthreshold slope of thin-film SOI MOSFETs. IEEE Electron Device Letters 2002;23.

[15] Kolarova R, Skotnicki T, Chroboczek JA. Low frequency noise in thin gate oxide MOSFETs. Microelectronics Reliability 2001;41:579–85. https://doi.org/10.1016/S0026-2714(00)00248-1.

[16] Ghibaudo G, Boutchacha T. Electrical noise and RTS fluctuations in advanced CMOS devices. Microelectronics Reliability 2002;42:573–82.

[17] Mercha A, Vandamme LKJ, Pichon L, Carin R, Bonnaud O. Current crowding and 1/f noise in polycrystalline silicon thin film transistors. J Appl Phys 2001;90:4019–26. https://doi.org/10.1063/1.1404418.

Journal Pre-proofs

- The variation of the buried channel position in the polysilicon thin film causes a second plateau in the $(g_m/I_D)^2$ curves for bias points in subthreshold region
- $1/f$ noise is confirmed as the main component of LFN in the subthreshold region of the studied SGTs.
- Carrier mobility fluctuation (CMF) is found to dominate the origin of LFN in TFT configuration and the low-current region of SGT.
- Carrier number fluctuation (CNF) is found to dominate the origin of LFN in the high-current region of SGT.

Journal Pre-proofs